A&A 441, 283–287 (2005)
DOI: 10.1051/0004-6361:20035742

Astronomy & Astrophysics

Discovery of a redshifted X-ray emission line in the symbiotic neutron star binary 4U 1700+24

A. Tiengo[1,2], D. K. Galloway[3], T. di Salvo[4], M. Méndez[5], J. M. Miller[6,7], J. L. Sokoloski[6,7], and M. van der Klis[8]

[1] Istituto di Astrofisica Spaziale e Fisica Cosmica, Sezione di Milano "G.Occhialini" – INAF, via Bassini 15, Milano 20133, Italy
e-mail: tiengo@mi.iasf.cnr.it
[2] Università degli Studi di Milano, Dipartimento di Fisica, via Celoria 16, 20133 Milano, Italy
[3] Center for Space Research, Massachusetts Institute of Technology, Cambridge, MA 02139-4307, USA
[4] Dipartimento di Scienze Fisiche ed Astronomiche, Università di Palermo, via Archirafi 36, 90123 Palermo, Italy
[5] SRON, National Institute for Space Research, Sorbonnelaan 2, 3584 CA, Utrecht, The Netherlands
[6] Harvard-Smithsonian Center for Astrophysics, 60 Garden Street, Cambridge, MA 02138, USA
[7] NSF Astronomy and Astrophysics Fellow
[8] Astronomical Institute "Anton Pannekoek", University of Amsterdam and Center for High-Energy Astrophysics, Kruislaan 403, 1098 SJ Amsterdam, The Netherlands

Received 25 November 2003 / Accepted 22 June 2005

Abstract. We present the spectral analysis of an *XMM-Newton* observation of the X-ray binary 4U 1700+24, performed during an outburst in August 2002. The EPIC-PN spectrum above 1 keV can be modeled by a blackbody plus Comptonization model, as in previous observations. At lower energies, however, we detect a prominent soft excess, which we model with a broad Gaussian centered at ∼0.5 keV. In the high resolution RGS spectrum we detect a single emission line, centered at $19.19^{+0.05}_{-0.09}$ Å. We discuss two possible interpretations for this line: O VIII at redshift $z = 0.012^{+0.002}_{-0.004}$ or Ne IX at redshift $z \sim 0.4$.

Key words. X-rays: individuals: 4U 1700+24 – stars: neutron – stars: binaries: symbiotic – line: identification

1. Introduction

Based on its optical identification with the M2 III giant HD154791 (Garcia et al. 1983; Masetti et al. 2002; also known as V934 Her), the X-ray source 4U 1700+24 is classified as both a Low Mass X-ray Binary (Liu et al. 2001) and a symbiotic-like binary (Garcia et al. 1983). The lack of signatures of binarity and the initially marginal positional coincidence (Morgan & Garcia 2001) originally made this identification uncertain. More recently, the detection of radial velocity variations from the proposed optical counterpart with the same period as X-ray brightness variations (Galloway et al. 2002) has added support to the identification.

In X-rays, 4U 1700+24 has long periods in which it is faint, and occasional episodes in which the flux increases by more than an order of magnitude. Assuming a distance of 420 pc (Masetti et al. 2002), the 2–10 keV luminosity of 4U 1700+24 varies from 2×10^{32}, which is much higher than expected from an isolated M giant of this spectral type, to 10^{34} erg s^{-1}. Masetti et al. (2002) reported the analysis of six observations from five different X-ray satellites, including an observation with the *Rossi X-Ray Timing Explorer* (*RXTE*; Jahoda et al. 1996) taken during a ∼100-day outburst in November 1997. Although no coherent pulsations or QPOs were detected, their analysis shows that the X-ray flux is also variable on short time scales (∼seconds).

In July 2002, the *RXTE* All-Sky Monitor light curve of 4U 1700+24 indicated that the source was undergoing a new outburst, and a Target of Opportunity observation was performed by the *XMM-Newton* satellite. In the following sections we discuss the analysis of the spectroscopic X-ray data from this observation.

2. Observations and data reduction

4U 1700+24 was observed with the *XMM-Newton* satellite (Jansen et al. 2001) on 2002 August 11. The *XMM-Newton* X-ray optics consist of three nested Wolter-I mirror assemblies, illuminating five X-ray detectors which operate simultaneously. CCDs sensitive to photons in the range 0.15−15 keV are situated at the focal point of each the three mirrors, two MOS and one PN types, comprising the *European Photon Imaging Camera* (EPIC, Strüder et al. 2001; Turner et al. 2001). Two of the mirrors also illuminate the *Reflection Grating Spectrometers* (RGS, den Herder et al. 2001) which disperse photons in the range 5–35 Å onto a pair of dedicated off-axis CCDs. The PN and MOS cameras have spectral resolutions of ≃80 eV and ≃70 eV (at 1 keV) and point spread functions

(PSFs) of ≃6″ and ≃5″ for the PN and MOS cameras, respectively. The RGS spectral resolution is 0.04 Å although it has a significantly smaller effective area (≃100 cm^2 at 1 keV for each of the two units, compared to ≃1200 cm^2 for the PN and ≃900 cm^2 for the sum of the two MOS detectors) and cannot produce 2-dimensional images.

The exposure time of the 4U 1700+24 observation (corrected for the dead-time) was 6 ks for the PN, 7 ks for the MOS, and 8 ks for the RGS. To avoid excessive optical loading on the PN and MOS cameras from the bright optical companion of 4U 1700+24 (V = 7.6), the "thick" filter was selected. The X-ray brightness of 4U 1700+24 during this high-state observation necessitated the use of Small Window operating mode, in which only a small portion (about 4′ × 4′ for the PN and 2′ × 2′ for the MOS) of the CCD is read out in a reduced frame time (6 ms for PN and 300 ms for MOS). The short readout time of this mode helps reduce errors due to photon pile-up, which occurs when two (or more) photons hit nearby pixels during a single CCD exposure, producing an event that is indistinguishable from a single, higher energy photon. The main effects of photon pile-up are an incorrect reconstruction of the event energies and an underestimation of the source count rate.

All the data were processed using the *XMM-Newton Science Analysis System* (SAS, version 6.1.0)[1]. The use of Small Window mode only partially mitigated the effects of pile-up[2] in the PN and MOS data, and so in our extraction of source photons we excluded the central part of the source PSF, where the incident count rate per pixel is the highest. The EPIC spectra were thus extracted from annular regions centered on the source, with inner and outer radii of 10″ and 40″, respectively. With these regions, we were able to completely remove the portion of the image affected by pile-up from the PN data, but not from the MOS data. The choice of an even larger inner radius for MOS would have greatly reduced the number of valid counts. Therefore, the MOS spectra are not discussed in this paper. To generate the PN spectrum, only single and double events were retained, and the resulting spectrum was rebinned both to have at least 30 counts in every energy channel and at most three bins per PN energy resolution element. A background spectrum was extracted from a region far enough from 4U 1700+24 to avoid contamination by source photons. In the 0.2–12 keV range, the background contributes less than 0.5% of the total count rate for most of the observation, increasing to 3% during the last 1500 s.

The RGS spectra (source and background) were extracted, and response matrices calculated using the standard reduction procedures. Since the source photons are widely spread along the dispersion axis, the RGS data are not affected by pile-up. The RGS source spectra were also rebinned in order to have at least 30 counts in every channel.

[1] `http://xmm.vilspa.esa.es/external/xmm_sw_cal/sas_frame.shtml`

[2] The presence of pile-up in a dataset can be investigated by examining the energy distribution of single, double, and multiple events (composed, respectively, of one, two, and greater than two adjacent pixels being above the detection threshold).

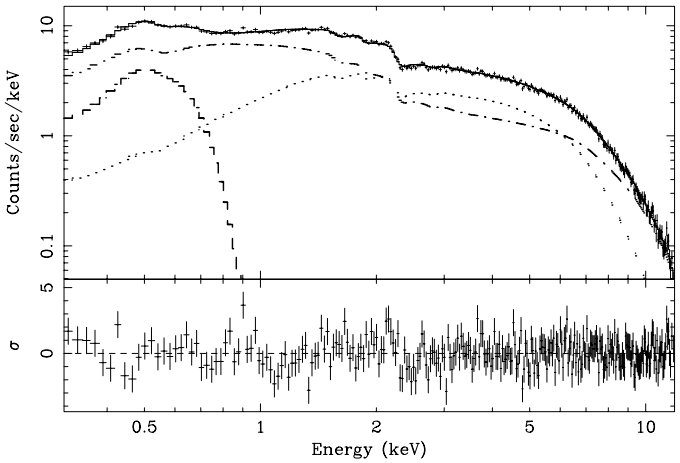

Fig. 1. The PN count rate spectrum of 4U 1700+24, and residuals (in units of σ) with respect to the best-fit model described in Table 1. The individual model components are also shown: dashed line for the broad Gaussian, dotted line for the blackbody and dash-dotted line for the Comptonization model.

3. Analysis and results

3.1. Spectral continuum

In order to compare the *XMM-Newton* spectrum of 4U 1700+24 with previous observations, we fitted the PN spectrum in the 0.3–12 keV range with the two-component model used by Masetti et al. (2002): a blackbody plus Comptonization (COMPST; Sunyaev & Titarchuk 1980), with absorption fixed to the Galactic value of $N_{\rm H} = 4 \times 10^{20}$ cm^{-2} (Dickey & Lockman 1990). The resulting fit is unacceptable ($\chi^2_{\rm red}$ = 4.05 for 273 degrees of freedom) due to a large excess at low energies. The fit can be improved by adding a component that contributes below ≃1 keV. We obtain the best results by modeling this soft excess with a broad ($\sigma \simeq 0.1$ keV) Gaussian line centered at ≃0.5 keV. We report the spectral parameters in Table 1. We show the PN spectrum and its residuals with respect to this model in Fig. 1. Although even our final fit is only marginally acceptable ($\chi^2_{\rm red}$ = 1.19 for 270 d.o.f., corresponding to a null hypothesis probability of 0.018), the addition of a systematic error of 1.5%, which is compatible with the current calibration uncertainties of the PN, reduces $\chi^2_{\rm red}$ to 1. No narrow features are detected in the PN spectrum. In particular, the 3σ upper limit on the equivalent width of a Fe K-α fluorescent line at 6.4 keV is ≃15 eV.

3.2. The emission line at 19.2 Å

The high spectral resolution of the RGS allows us to search for narrow features in the X-ray spectrum of 4U 1700+24 at low energies. In Fig. 2, we show the first-order RGS spectrum of 4U 1700+24 and residuals with respect to the best-fit model derived from analysis of the PN data. In addition to some deviations from the continuum model due to problems in the cross-calibration between the PN and RGS instruments (Kirsch et al. 2004), an emission line is apparent at about 19 Å (Fig. 2). The addition of a Gaussian component in the model

Table 1. Best fit parameters of the PN spectrum in the 0.3–12 keV energy range. Errors are at the 3σ confidence level for a single interesting parameter.

$N_{\rm H}$ (10^{20} cm^{-2})	4 (fixed)
$kT_{\rm e}$ (keV)	$4.4^{+2.8}_{-0.9}$
τ	$18.5^{+1.7}_{-5.0}$
$N_{\rm C}^{(a)}$	0.0229 ± 0.0007
$kT_{\rm BB}$ (keV)	1.40 ± 0.03
$R_{\rm BB}$ (m)$^{(b)}$	113 ± 3
$E_{\rm line}$ (eV)	505^{+13}_{-12}
σ (eV)	112^{+25}_{-20}
Equivalent width (eV)	198^{+34}_{-28}
$\chi^2_{\rm red}$ (d.o.f.)	1.188 (270)
0.3–2 keV flux$^{(c)}$	8.4×10^{-11}
2–10 keV flux$^{(c)}$	5.3×10^{-10}

$^{(a)}$ Normalization of the COMPST model in XSPEC version 11.3.
$^{(b)}$ Radius at infinity assuming a distance of 420 pc.
$^{(c)}$ Absorbed flux in units of ergs cm^{-2} s^{-1}.

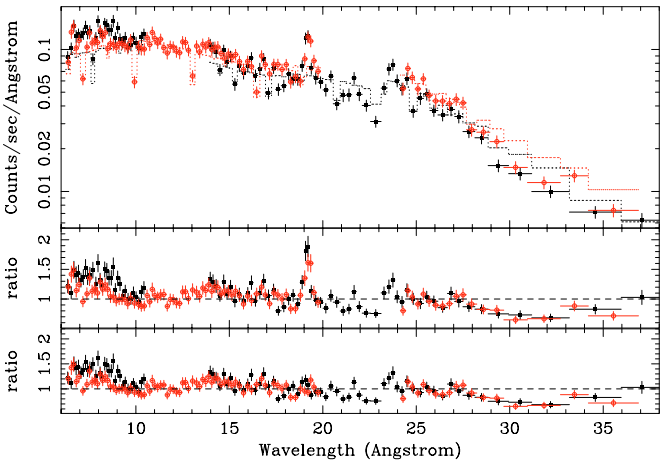

Fig. 2. RGS1 (filled squares) and RGS2 (open circles) spectra of 4U 1700+24. The residuals in the middle panel are relative to the model derived from the PN data analysis (see Table 1) multiplied by a factor 0.8 to account for the discrepancies in flux estimates between the PN and RGS. The lower panel shows the residuals relative to the same model plus an emission line at 19.19 Å. For clarity, the data have been rebinned to a bin size larger than the RGS energy resolution. The data gaps at 10.5–14 Å for RGS1 and 20–24 Å for RGS2 correspond to the CCDs lost due to electronic failure in the early phase of the mission.

accounts for the residuals in this region of the spectrum (see bottom panel of Fig. 2) and improves the χ^2 from 1.65 (for 765 d.o.f.) to 1.54 (for 762 d.o.f.). The emission-line parameters are: $\lambda = 19.19^{+0.05}_{-0.09}$ Å, $\sigma = 3.9^{+2.7}_{-1.3}$ eV, line flux equals $(4.9^{+1.9}_{-1.6}) \times 10^{-4}$ photons cm^{-2} s^{-1}, and equivalent width equals $9.7^{+3.8}_{-3.1}$ eV (all the quoted errors are 3σ errors).

In the X-ray atomic lines catalogue ATOMDB 1.3.1[3], only very low emissivity transitions are found within 3σ of the line position; most are satellite lines of H-like and He-like oxygen, with a maximum emissivity of 8.4×10^{-18} photons cm^3 s^{-1}. The Ly-ϵ line of N VII (which is not included in the ATOMDB database) has a wavelength compatible with the observed emission line ($\lambda = 19.118$ Å, Verner et al. 1996a), but the probability for this transition is very low. The Ly-α transition of H-like oxygen (O VIII) has an emissivity more than 2 orders of magnitude higher than that of the lines mentioned above (which makes it typically one of the strongest lines found in cosmic X-ray sources) and a rest-frame wavelength of 18.97 Å, slightly smaller than the value we find for the emission line shown in Fig. 2. It is therefore possible that the X-ray emission line in 4U 1700+24 is O VIII at redshift $z = 0.012^{+0.002}_{-0.004}$.

The accuracy of the RGS wavelength scale is better than 10 mÅ (Pollock 2004), with an additional 2.3 mÅ of systematic error for each arcsecond error in the pointing or source coordinates. For the 4U 1700+24 observation, the additional error is smaller than 10 mÅ, since the EPIC positional accuracy is better than 4″ and the RGS data were processed using source coordinates derived from the EPIC images. Therefore, we exclude the possibility that the wavelength shift from the O VIII rest-frame position is due to an incorrect wavelength scale in the RGS instrument.

Other smaller structures are also present in the residuals. In particular, the data differ substantially from the model around the instrumental oxygen edge at ≃23.5 Å, where the RGS effective area calibration is complex. We can improve the RGS spectral fit slightly ($\chi^2_{\rm red} = 1.51$ for 761 d.o.f.) by including an overabundance of neutral oxygen in the photoelectric absorption model (with cross section from Verner at al. 1996b). Keeping the hydrogen column density fixed at the value of 4×10^{20} cm^{-2}, we obtain a best-fit value for the oxygen abundance of $2.0^{+0.3}_{-0.5}$ times the solar value (Anders & Grevesse 1989). On the other hand, two instrumental absorption features at 23.05 and 23.35 Å contribute $\sim 2 \times 10^{17}$ cm^{-2} to the oxygen column density (de Vries et al. 2003) and could also explain most of the detected overabundance of oxygen.

If the emission line at 19.19 Å is redshifted O VIII, we might expect spectral features from other ionization states of oxygen. The signature of He-like oxygen is a triplet of X-ray lines at 21.6, 21.8, and 22.1 Å. Some residuals are in fact present in the RGS spectrum around 21.8 Å, which corresponds to either the rest-wavelength of the intercombination line or a resonance line at $z = 0.01$. Fitting the residuals at 21.8 Å with a Gaussian of the same width as the O VIII line candidate ($\sigma = 4$ eV) gives a 3σ upper limit for the equivalent width of 5 eV. Fully ionized oxygen should produce an O VIII radiative recombination continuum at around 14 Å (14.2 Å for plasma at rest and 14.4 Å at $z = 0.01$). The RGS spectrum shows some residuals at this location. Including a recombination emission edge at 14.4 Å with a 50 eV width in the fit gives a normalization of $(6.1 \pm 3.1) \times 10^{-4}$ photons cm^{-2} s^{-1}. The addition of this component is statistically significant, although it is quite broad and could also result from uncertainties in the spectral continuum model. The RGS spectra were also rebinned using different criteria, but no other spectral features could be identified.

[3] http://asc.harvard.edu/atomdb/

Due to the poorer energy resolution of the PN camera, no line at 19.19 Å is significantly detected in the PN data. However, if we fix the energy and the width of the line to the values derived from the RGS data, the upper limit to the line equivalent width is 12 eV, which is consistent with the RGS results.

4. Discussion

The high sensitivity of *XMM-Newton* at low energies and the high spectral resolution of the RGS instrument have revealed new features in the X-ray spectrum of the unusual interacting binary 4U 1700+24. Although the PN spectrum above 1 keV is consistent with the rather variable spectra seen in previous observations (Masetti et al. 2002), we clearly detect both a soft excess and an emission line at 19.2 Å.

The best fit to the soft excess was found by adding a broad Gaussian line component to the high-energy continuum model (blackbody + Comptonization). But the interpretation of this feature as an emission line is problematic. No strong emission lines are expected at the wavelength of the soft excess for either $z = 0.01$ or $z = 0$. In addition, both the intensity and broadening of this line would be much larger than for the line at 19.2 Å.

As mentioned above, we have also discovered an emission line at 19.2 Å. Since only very low emissivity lines are consistent with the observed wavelength of $\lambda = 19.19^{+0.05}_{-0.09}$ Å, the line may be O VIII at redshift ≃0.01. For most high-emissivity lines close to this wavelength, a much larger redshift/blueshift would be required. For example, among the other strong lines expected in the spectrum of an accreting X-ray binary, the O VII and Ne IX triplets are the nearest candidates for the line identification, at longer and shorter wavelengths, respectively. For O VII, the line would be blue-shifted by a factor > 0.1, which, in case of Doppler shift, requires that the emitting plasma is moving towards us at more than 10% of the speed of light. On 2002 July 29 radio observations were performed to look for a possible jet, but no source was detected with an upper limit of 1.0 ± 0.7 mJy at 15 GHz (G. Pooley 2002, private communication).

On the other hand, the identification of the line at 19.2 Å with the Ne IX triplet would imply redshifts of 0.40, 0.41, and 0.42 for the forbidden, intercombination and resonance lines, respectively. These values could be interpreted as gravitational redshift from close to the surface of a neutron star, as they are consistent with most of the equations of state for neutron stars composed of normal nuclear matter, and they are just slightly larger than the redshift $z = 0.35$ found by Cottam et al. (2002) in the spectral analysis of X-ray bursts from EXO 0748–676. However, due to the lack of identifications of other spectral features at $z \sim 0.4$ or indication for overabundance of neon, we consider O VIII to be a better candidate for the observed emission line.

The relatively small redshift of the O VIII line ($z \simeq 0.01$) can be interpreted in several ways, and we briefly discuss two possible scenarios. A value of $z = 0.008–0.014$ corresponds to the gravitational redshift of a photon emitted at a distance of 35–60 Schwarzschild radii from a compact object: this interpretation would exclude the possibility that 4U 1700+24 is a white dwarf and would correspond to a distance of $1.5–2.6 \times 10^7$ cm from a 1.4 $M_\odot$ neutron star. In a photoionized plasma, assuming that most of the oxygen is H-like, the measured O VIII line luminosity of $\simeq 10^{40}$ photons s^{-1} gives an emission measure of $EM \simeq 6 \times 10^{53}$ cm^{-3} (taking an abundance of $\simeq 1.6 \times 10^{-3}$, as derived from the oxygen edge fit and assuming that the overabundance is intrinsic to the X-ray source). Assuming a spherically symmetric geometry, if the O VIII line is emitted at $\simeq 2 \times 10^7$ cm from the neutron star, we can estimate a density of $n \simeq 4 \times 10^{15}$ cm^{-3}. For the measured continuum luminosity of 10^{34} erg s^{-1}, the ionization parameter is $\xi = L_{\rm cont}/(nR^2) \simeq 5000$ erg cm s^{-1}. For such a high ionization parameter, most of the oxygen should be fully ionized and therefore we would not expect to see a prominent O VIII emission line. O VIII dominates the ionization states of oxygen for $\xi \simeq 100$ erg cm s^{-1}, which means that either we have used an oversimplified model (assuming, for example, that the line emission region is symmetric and homogeneous) or that the O VIII line is emitted at larger distance from the central X-ray source and therefore that the redshift is not solely gravitational.

In an alternative scenario, the same redshift can be produced by Doppler effects if the emitting plasma is moving away from us at a speed of 2000–4000 km s^{-1}. This velocity is about two orders of magnitude larger than the wind velocity of an M-type giant (Reimers 1977), as well as the proper motion and possible orbital velocity of the binary system (Galloway et al. 2002). Although the high luminosity, hard X-ray spectrum, and rapid X-ray variability of 4U 1700+24 make it rather unlikely, the present data do not rule out the possibility that the accreting object is a white dwarf. The detection of Doppler-shifted lines of highly ionized elements has been reported for some supersoft sources and interpreted as the signature of collimated outflows ("jets") coming from the accreting white dwarf (e.g., Cowley et al. 1998). Furthermore, the jet velocity is typically similar to the value we derive for the redshifted O VIII line. In our case, however, no corresponding blueshifted line is detected, which implies either a unipolar jet or some special geometry to obscure the approaching jet.

For a neutron star with a 10^{12} gauss magnetic field and a luminosity of 10^{34} erg s^{-1}, the magnetospheric radius is $\simeq 3 \times 10^9$ cm (Hayakawa 1985). Although X-ray pulsations have not been found from 4U 1700+24, the fact that it is probably viewed close to face-on (Galloway et al. 2002) means that pulsations would be undetectable even if it is an accreting neutron star with high magnetic field as the line of sight is almost aligned with the neutron star spin axis. At a distance of $\simeq 3 \times 10^9$ cm from a 1.4 $M_\odot$ neutron star, a free particle would move radially towards the neutron star with a velocity of ≃3400 km s^{-1}. Therefore, the redshift we measure could originate from close to the magnetospheric radius, where the plasma density is increased by the funneling effect produced by the magnetic field lines. Repeating the estimates of the ionization parameter described above, at a distance of 3×10^9 cm the corresponding density is $n \simeq 2 \times 10^{12}$ cm^{-3} and $\xi \simeq 500$. These two values are fairly consistent with the presence of an O VIII line.

Redshifted emission lines have also been reported in Cygnus X-3. Paerels et al. (2000) reported a redshift

corresponding to 750–800 km s^{-1} for all the emission lines detected in a *Chandra* HETGS observation of Cygnus X-3. In two more recent *Chandra* observations, a slightly smaller redshift of 270–550 km s^{-1}, in addition to a Doppler modulation of about 150 km s^{-1}, was found (Stark & Saia 2003). The second effect was interpreted as being due to the binary orbital motion, but no convincing explanation was given for the global redshift. Although the X-ray luminosities and observed redshifts of 4U 1700+24 and Cygnus X-3 are rather different, a common mechanism could produce the line redshifts. For both 4U 1700+24 and Cygnus X-3, a low orbital inclination has been proposed (Galloway et al. 2002; Mioduszewski et al. 2001). Thus, Doppler shifts due to the bulk velocity of matter receding from us as it falls onto the compact object could be the origin of the redshifted lines.

Acknowledgements. Based on observations obtained with XMM-Newton, an ESA science mission with instruments and contributions directly funded by ESA Member States and NASA. This work was partially supported by the Netherlands Organization for Scientific Research (NWO). This work was supported in part by the NASA Long Term Space Astrophysics program under grant NAG 5-9184. JMM and JLS gratefully acknowledge support from the NSF.

References

Anders, E., & Grevesse, N. 1989, Geochimica et Cosmochimica Acta, 53, 197
Cottam, J., Paerels, F., & Méndez, M. 2002, Nature, 420, 51
Cowley, A. P., Schmidtke, P. C., Crampton, D., & Hutchings, J. B. 1998, ApJ, 504, 854
de Vries, C. P., den Herder, J. W., Kaastra, J. S., et al. 2003, A&A, 404, 959
den Herder, J. W., Brinkman, A. C., Kahn, S. M., et al. 2001, A&A, 365, L7
Dickey, J. M., & Lockman, F. J. 1990, ARA&A, 28, 215
Galloway, D. K., Sokoloski, J. L., & Kenyon, S. J. 2002, ApJ, 580, 1065
Garcia, M., Baliunas, S. L., Elvis, M., et al. 1983, ApJ, 267, 291
Hayakawa, S. 1985, Phys. Rep., 121, 317
Jahoda, K., Swank, J. H., Giles, A. B., et al. 1996, SPIE, 2808, 59
Jansen, F., Lumb, D., Altieri, B., et al. 2001, A&A, 365, L1
Kirsch, M. G. F., Altieri, B., Chen, B., et al. 2004, SPIE, 5488, 103
Liu, Q. Z., van Paradijs, J., & van den Heuvel, E. P. J. 2001, A&A, 368, 1021
Masetti, N., Dal Fiume, D., Cusumano, G., et al. 2002, A&A, 382,104
Mioduszewski, A. J., Rupen, M. P., Hjellming, R. M., Pooley, G. G., & Waltman, E. B. 2001, ApJ, 553, 766
Morgan, W. A., & Garcia, M. R. 2001, PASP, 113, 1386
Paerels, F., Cottam, J., Sako, M., et al. 2000, ApJ, 533, L135
Pollock, A. M. T. 2004, RGS Status of calibration and data analysis, `http://xmm.vilspa.esa.es/external/xmm_sw_cal/calib/index.shtml`
Reimers, D. 1977, A&A, 57, 395
Stark, M. J., & Saia, M. 2003, ApJ, 587, L101
Strüder, L., Briel, U., Dennerl, K., et al. 2001, A&A, 365, L18
Sunyaev, R. A., & Titarchuk, L. 1980, A&A, 86, 121
Turner, M. J. L., Abbey, A., Arnaud, M., et al. 2001, A&A, 365, L27
Verner, D. A., Verner, E. M., & Ferland, G. J. 1996a, At. Data Nucl. Data Tables, 64, 1
Verner, D. A., Ferland, G. J., Korista, K. T., & Yakovlev, D. G. 1996b, ApJ, 465, 487